




RESEARCH ARTICLE

Polyacrylamide-based hydrogel coatings improve biocompatibility of implanted pump devices

Doreen Chan^{1,2} | Caitlin L. Maikawa^{2,3}  | Andrea I. d'Aquino²  |
Shyam S. Raghavan⁴ | Megan L. Troxell⁵ | Eric A. Appel^{2,3,6,7,8} 

¹Department of Chemistry, Stanford University, Stanford, California, USA

²Department of Materials Science & Engineering, Stanford University, Stanford, California, USA

³Department of Bioengineering, Stanford University, Stanford, California, USA

⁴Department of Pathology, Stanford University School of Medicine, Stanford, California, USA

⁵Department of Pathology, University of Virginia, Charlottesville, Virginia, USA

⁶Department of Pediatrics (Endocrinology), Stanford University School of Medicine, Stanford, California, USA

⁷Woods Institute for the Environment, Stanford University, Stanford, California, USA

⁸ChEM-H Institute, Stanford University, Stanford, California, USA

Correspondence

Eric A. Appel, Department of Materials Science & Engineering, Stanford University, Stanford, CA 94305, USA.
Email: eappel@stanford.edu

Funding information

American Diabetes Association, Grant/Award Number: 1-18-JDF-011; National Institute of Diabetes and Digestive and Kidney Diseases, Grant/Award Numbers: P30DK116074, R01DK119254

Abstract

The introduction of transcutaneous and subcutaneous implants and devices into the human body instigates fouling and foreign body responses (FBRs) that limit their functional lifetimes. Polymer coatings are a promising solution to improve the biocompatibility of such implants, with potential to enhance in vivo device performance and prolong device lifetime. Here we sought to develop novel materials for use as coatings on subcutaneously implanted devices to reduce the FBR and local tissue inflammation in comparison to gold standard materials such as poly(ethylene glycol) and polyzwitterions. We prepared a library of polyacrylamide-based copolymer hydrogels, which were selected from materials previously shown to exhibit remarkable antifouling properties with blood and plasma, and implanted them into the subcutaneous space of mice to evaluate their biocompatibility over the course of 1 month. The top performing polyacrylamide-based copolymer hydrogel material, comprising a 50:50 mixture of *N*-(2-hydroxyethyl)acrylamide (HEAm) and *N*-(3-methoxypropyl)acrylamide (MPAm), exhibited significantly better biocompatibility and lower tissue inflammation than gold standard materials. Moreover, when applied to polydimethylsiloxane disks or silicon catheters as a thin coating ($45 \pm 1 \mu\text{m}$), this leading copolymer hydrogel coating significantly improved implant biocompatibility. Using a rat model of insulin-deficient diabetes, we showed that insulin pumps fitted with HEAm-co-MPAm hydrogel-coated insulin infusion catheters exhibited improved biocompatibility and extended functional lifetime over pumps fitted with industry standard catheters. These polyacrylamide-based copolymer hydrogel coatings have the potential to improve device function and lifetime, thereby reducing the burden of disease management for people regularly using implanted devices.

KEYWORDS

biocompatibility, diabetes, foreign body response, hydrogels, insulin pump

1 | INTRODUCTION

Remarkable progress has been made over the past few decades on long-term implantable devices such as cardiac pacemakers, hernia meshes, and dental and heart implants, which has improved patient

health across numerous disease indications. The worldwide medical device industry is estimated to be \$150 billion¹ and uses materials fabricated with metals (e.g., titanium, nitinol, and stainless steel²) or soft materials (e.g., polytetrafluoroethylene, silicones, poly[ethylene terephthalate], among others³). It is desirable for these materials to be

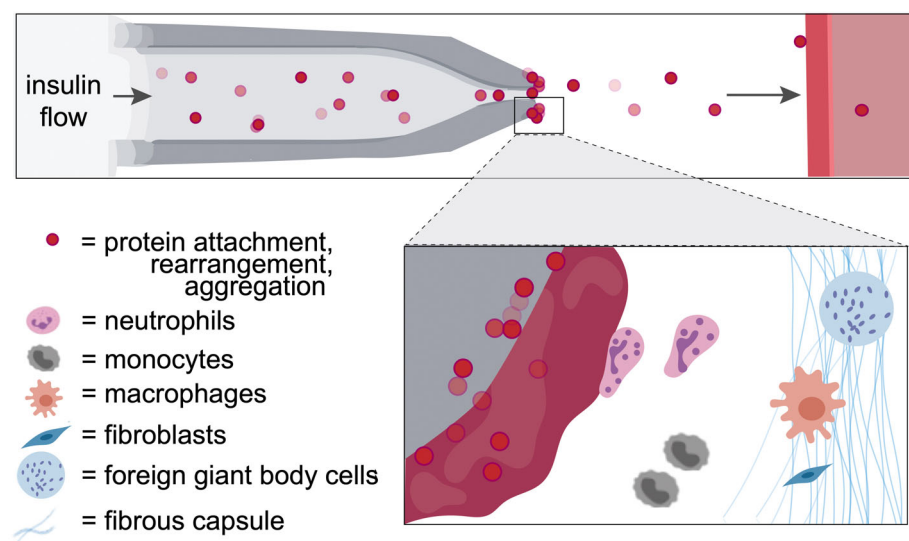


FIGURE 1 Schematic of the foreign body response to an insulin infusion set. Protein aggregation and innate immune cell activation at the catheter tip of subcutaneously implanted pumps for continuous insulin infusion leads to a cascading foreign body responses that result in device failure, requiring changing of the insulin infusion set.

biocompatible, as these devices are designed to integrate and function with the human body. Unfortunately, for temporary implantable devices and biosensors such as glucose monitors, insulin pumps, catheters, and neural probes, these immune responses are typically undesirable as they inhibit device performance, shorten device lifetime, cause scarring in the local tissues, and result in a requirement for frequent device replacement.^{1,4}

Upon implantation, materials and devices form a complex interface with tissues⁵ and their surface is instantaneously coated with proteins such as fibrinogen, IgG, fibronectin, and von Willebrand factor.⁵ While the link between fouling and biocompatibility is still poorly understood,⁶ it has been generally agreed upon that protein adhesion is the first step in fouling. Upon adsorption, proteins undergo conformational changes, and the protein fouled surface is activated. Following protein fouling is the infiltration of neutrophils (acute inflammation), recruitment of macrophages and monocytes (chronic activation), and cell fusion to form foreign body cells. This process is enhanced by secretion of soluble factors and collagen production by fibroblasts (Figure 1). These factors contribute ultimately to the foreign body response (FBR) and acute inflammatory response that dictates how surrounding immune cells respond, including attracting other cells or masking the foreign material.⁷ This process is dynamic as cells, especially macrophages, are recruited to the implanted materials and devices and secrete more proteins and respond directly to the foreign material. Over time, fibroblasts secrete collagen fibrils on the surface of these implanted materials and devices that results in the formation of a fibrous capsule that is avascular, impermeable to cells, hinders metabolite transport, and serves to isolate the material from the body. This fibrotic response to implanted materials ultimately compromises long-term function of implantable materials and devices.^{8,9}

Devices used for effective management of type I diabetes mellitus (T1D) are particularly strongly affected by the immune system and resulting FBR.^{10,11} People with diabetes rely on continuous glucose monitors (CGMs) to evaluate glucose levels in real time, as well as

insulin pumps to provide basal and bolus infusions of insulin to manage blood glucose. Both devices utilize a catheter tip that is implanted in the subcutaneous space of the patient's abdomen. While insulin pumps face many technical challenges, such as battery life and viability of insulin on board, the most burdensome challenge for their effective use is occlusion of the infusion set catheter tips on account of the FBR.¹¹ Indeed, aggregation of administered insulin at the catheter tip encourages and exacerbates the FBR, resulting in occlusion and flow irregularities. For many insulin drug products, infusion sets are recommended to be removed and replaced at a new site in the patient's abdominal subcutaneous tissue at a minimum of every 3 days. This highly burdensome process leads to noncompliance among those with diabetes, and people who use infusion sets for longer than the recommended period can experience irritation at the insertion site and inconsistent insulin delivery resulting in poor disease management.¹⁰ Thus, there is a strong motivation to improve the biocompatibility of the inserted catheter tips to mitigate occlusion and extend the lifetime of these crucial devices.

To address the shortcomings of current infusion set catheters, significant efforts toward surface and bulk modifications have been made to these implanted devices.^{5,12} In particular, antifouling polymeric brush and hydrogel coatings are an attractive option for surface modification, as they serve to mediate the interface between implanted materials and the body. These modifications can be designed to prevent adsorption of proteins and preclude infiltration of immune cells to reduce the severity of the FBR.^{13,14} Notably, hydrogels comprising zwitterionic monomers such as poly(2-methacryloyloxyethyl phosphorylcholine) (PMPC) have been shown to exhibit a high degree of biocompatibility,^{15,16} and PMPC-based polymer brushes have demonstrated an ability to improve performance and reduce noise on CGMs due to robust surface hydration arising from strong intermolecular bond formation between the charges on the polymers and surrounding water molecules.¹⁷ Similarly, poly(ethylene glycol) (PEG) is often regarded as the gold standard polymer for antifouling coatings.^{6,18–20} Unfortunately, due to rising concerns of PEGs immunogenicity and recent research

demonstrating that both PEG and PMPC exhibit poor long-term stability,²¹⁻²³ there is growing interest in the discovery and development of new classes of antifouling materials. Recently, polyacrylamide-based copolymer hydrogel coatings have been reported which exhibit excellent antibiofouling properties and stability.²⁴ In this work, we investigate a series of antifouling polyacrylamide-based copolymer hydrogel materials to identify coating materials that reduce the FBR to implanted materials, including catheters on insulin pumps. We show that select hydrogel formulations mitigate the FBR and improve the functional lifetime of implanted insulin pump devices.

TABLE 1 Table of combinatorial polyacrylamide copolymer hydrogel formulations evaluated.

Formulation	Monomer 1	Monomer 2
A1	10% HEAm	10% DEAm
A2	15% HEAm	5% DEAm
B3	10% ALMP	10% DMAM
C4	5% ALMP	15% MPAm
D5	10% HEAm	10% MPAm
E6	15% MPAm	5% Am
D7	15% HEAm	5% MPAm
F8	10% Am	10% DEAm
F9	10% Am	10% DEAm
G10	15% Am	5% tHMAM
H11	15% AMPSAm	5% Am
F12	15% Am	5% DEAm
I13	15% NiPAm	5% DMAM
J14	5% ALMP	15% MPAm
K15	10% DMAM	10% ALMP

Note: Binary mixtures of acrylamide monomers were used to prepare hydrogels (20 wt % solids).

2 | RESULTS

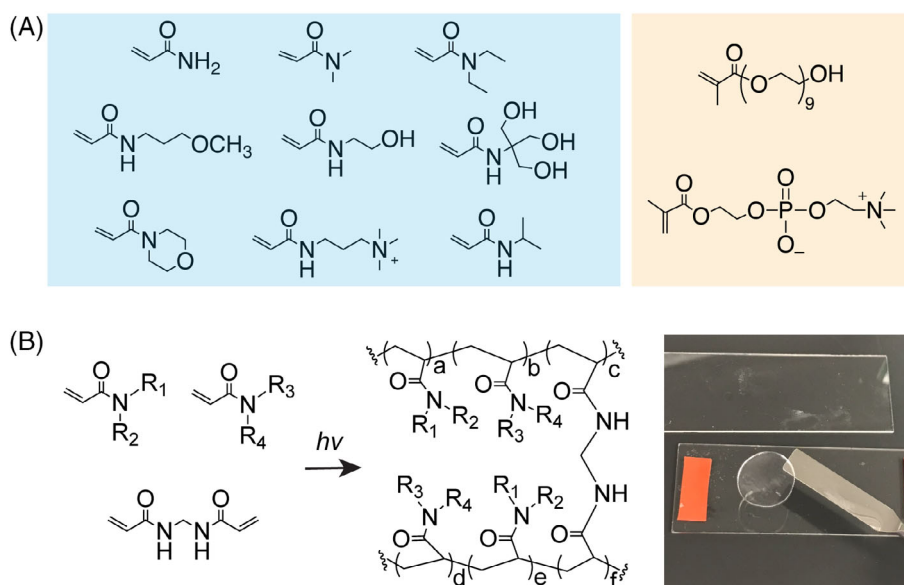
2.1 | Selection and synthesis of polyacrylamide hydrogels

From a recent study evaluating a large library of polyacrylamide-based copolymer hydrogels for their ability to prevent fouling by blood proteins and platelet adhesion,²⁵ we selected the top 15 antifouling formulations (Table 1, Figure S1) to compare their biocompatibility following subcutaneous implantation in mice against PEG and zwitterionic PMPC hydrogel formulations (Figure 2A). Each of these hydrogels can be prepared by photo-polymerization in a facile manner to yield a library of hydrogel disks with mechanical properties which can be tuned to be suitable for interfacing with the body. While we primarily investigated the top 15 antibiofouling formulations from the previously reported screen of platelet fouling,²⁵ a subset of randomly selected polyacrylamide-based copolymer hydrogels exhibiting varying levels of antifouling and platelet adhesion behavior were also synthesized and evaluated (Figure S2).

2.2 | Biocompatibility of polyacrylamide hydrogels

As the FBR severely hinders in vivo performance of implanted devices, we first sought to evaluate the FBR to each member of our hydrogel library and gold standard controls. For these initial screening studies, which were designed to identify trends in coating performance and identify leading candidate formulations for subsequent studies, a sample size of $N = 3$ provides sufficient study power. To screen these materials, we implanted hydrogel disks in the subcutaneous tissue in the dorsal region of a mouse. After 28 days, no mice showed signs of discomfort or distress, and implanted hydrogels and surrounding tissues were retrieved for histological analysis (Figure 3A). One measure of the FBR is quantification of the thickness

FIGURE 2 Polyacrylamide copolymer hydrogels to combat the foreign body response. (A) (left to right) acrylamide (Am); *N,N*-dimethylacrylamide (DMAM); *N,N*-diethylacrylamide (DEAm); *N*-(3-methoxypropyl)acrylamide (MPAm); *N*-(2-hydroxyethyl)acrylamide (HEAm); *N*-[tris(hydroxymethyl)methyl]acrylamide (tHMAM); 4-acryloylmorpholine (ALMP); *N*-[3-(dimethylamino)propyl] methacrylamide; 2-acrylamido-2-methylpropane sulfonic acid (AMPSAm); *N*-isopropylacrylamide (NiPAm). Poly(ethylene glycol) methacrylate and PMPC as controls. (B) Polymerization of acrylamide monomers are synthesized in a high-throughput manner.



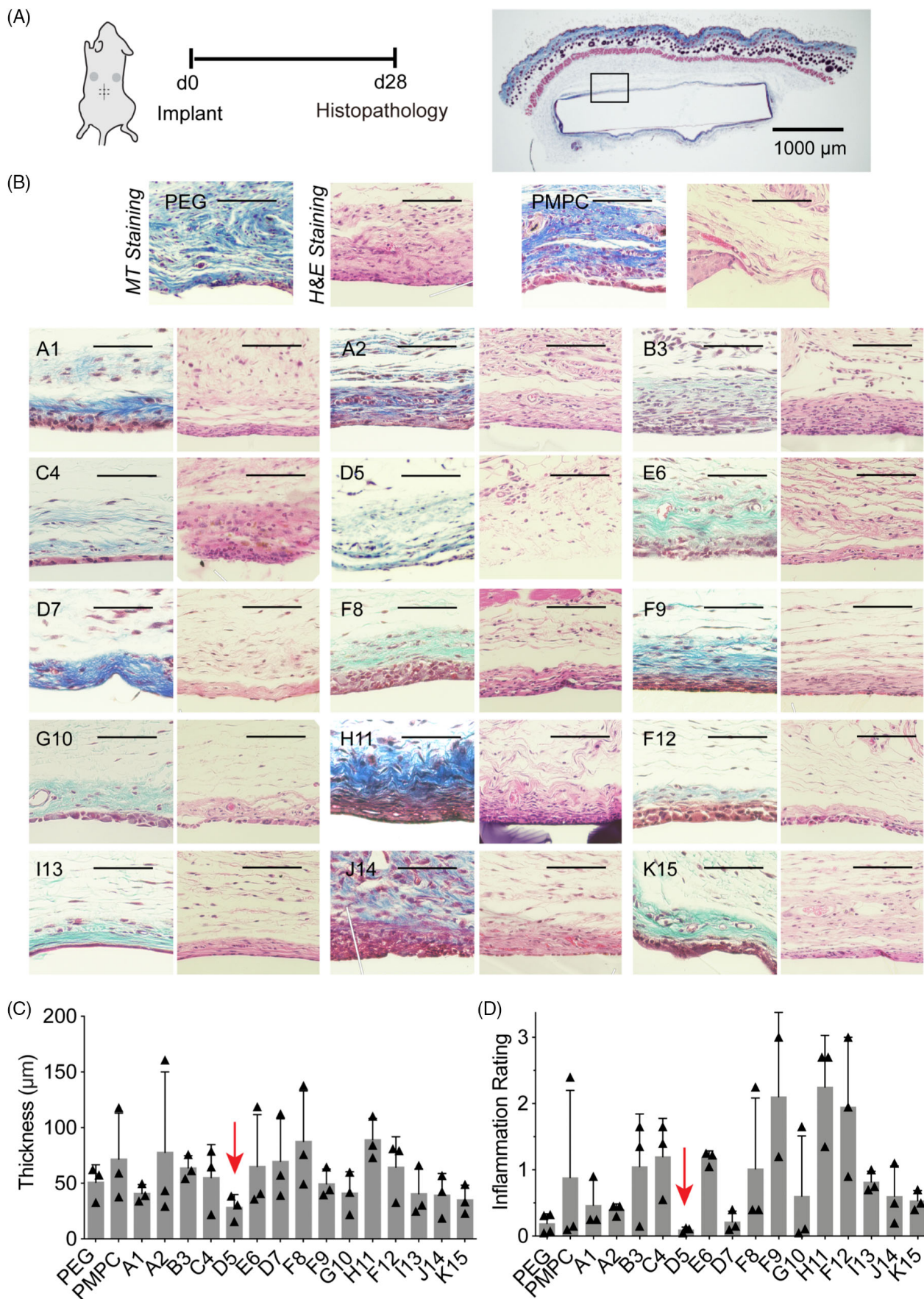


FIGURE 3 Legend on next page.

of the collagenous fibrous capsules surrounding implanted materials. After 28 days, excised tissues were processed and stained with Masson's Trichrome (MT) for evaluation (Figure 3B). With MT staining, collagenous fibrosis stains blue, edema and loose fibrosis stains pale blue, and more organized, dense fibrosis stains darker shades. By contrast, cells generally counterstain red, including inflammatory cells and macrophages that are part of the pseudosynovial layer.¹⁸ Capsule thickness quantification highlighted that a copolymer hydrogel formulation comprising 10 wt % *N*-(2-hydroxyethyl)acrylamide (HEAm) and 10 wt % *N*-(3-methoxypropyl)acrylamide (MPAm) (50:50 ratio of HEAm:MPAm) elicited the thinnest capsule layer ($28 \pm 11 \mu\text{m}$) while gold-standard polymers including PEG ($51 \pm 16 \mu\text{m}$) and PMPC ($72 \pm 41 \mu\text{m}$) elicited much more severe capsule formation (Figure 3C).

As fibrous capsule formation provides only one aspect of the FBR, we then investigated what cell types were recruited to the implants as well as the intensity of inflammation near the implants. Excised tissues were then stained with hematoxylin and eosin (H&E), where proteins (e.g., extracellular matrix deposition) stains pink, while nucleic acids (particularly cell nuclei) stains purple (Figure 3B). In all formulations, fibrous capsules were found to be lined by multilayered collections of histiocytes, forming a pseudo-synovium around the implanted materials. The immune cells surrounding both PEG and PMPC hydrogels were predominantly macrophages. In select copolymer hydrogel formulations such as J14, sparse chronic inflammation including plasma cells, lymphocytes and macrophages were present in the stroma deep to the capsule.²⁰ The presence of neutrophils indicates acute inflammation and was observed to correlate with more severe inflammatory infiltrates, admixed with macrophages and lymphocytes. For hydrogel sample H11, for example, cell presence was dominated by macrophages and neutrophils. By contrast, copolymer hydrogel formulation D5 exhibited few chronic inflammatory cells in stroma, and rare plasma cells and macrophages. A semiquantitative metric was used to assess the degree of inflammation (neutrophils, lymphocytes, plasma cells, monocytes, giant cells, not including the pseudosynovium) around the hydrogels. For this evaluation, the intensity of inflammation was assigned a score of 0 (none), 1 (mild), 2 (moderate), or 3 (severe inflammation), which was multiplied by the estimated percent of capsule circumference involved by inflammation. Pathologists blinded to the samples scored hydrogel formulation D5 with the lowest inflammation score of all of the materials evaluated: 0.10 ± 0.04 (Figure 3D). By contrast, gold standard materials PEG (0.19 ± 0.15) and PMPC (0.8 ± 1.1) exhibited higher and more variable inflammatory responses. These results indicate that the leading polyacrylamide copolymer hydrogel coating D5 exhibited notably improved biocompatibility over gold standard materials PEG and PMPC.

2.3 | Application of hydrogel coating to PDMS surface

In the body, proteins readily attach to the hydrophobic surface of polydimethylsiloxane (PDMS), a widely used implant material found in catheters, gastric bands, and breast implants.^{19,25} As a proof-of-concept for the applicability of our polyacrylamide-based copolymer hydrogels as coatings on implanted materials, we applied this hydrogel formulation to a PDMS substrate. Despite prevalent use as a biomaterial historically, these silicone-based materials have been subject of renewed controversy.²⁶⁻²⁹ Here, PDMS disks were first treated with 3-(trimethoxysilyl)propyl methacrylate (TMSPMA), and then a thin layer of prepolymer solution of D5, our top performing formulation, was applied by spin-coating and photo-crosslinked to form a robust hydrogel coating, which was characterized by scanning electron microscopy (SEM) to be $45 \pm 1 \mu\text{m}$ in thickness (Figure 4A). Considerably less platelet adhered was observed on the surface of the D5-coated PDMS disks than on bare disks when subjected to platelet-rich plasma (PRP) (Figure S4).

We then implanted hydrogel-coated and uncoated (bare) PDMS samples into the subcutaneous of mice. After 28 days, the implanted materials and surrounding tissues were harvested for histological analysis. MT and H&E staining was performed on samples from these implants (Figure 4B), demonstrating that the D5 hydrogel coating mitigated fibrous capsule formation ($p = .005$) and reduced the pathological inflammation score for these materials (Figure 4C). In this study, we used a sample size sufficiently large to provide adequate statistical power for head-to-head comparison of coated and uncoated substrates. In general, the primary reason for high study power is to lower the probability of type II error (a false negative result). Our analyses identify statistical significance in our results, thus precluding the possibility of type II error and implying that even with a relatively low sample size the observed effect size was sufficiently large that the probability of observing these results by chance was low enough to reject the null hypothesis. Post hoc power analysis (two-sample t test power calculation; effect size 20.8; standard deviation 5.1) supports these observations as the sample size required to achieve 80% power and a significance level of 0.05 in this study is 2.4 mice/group, which would be rounded up to $N = 3$ mice/group.

2.4 | Extending lifetime of osmotic insulin pumps

To whether these novel polyacrylamide-based copolymer hydrogel coatings can improve the functional lifetime of insulin pumps, we used implantable osmotic Alzet[®] pumps. These infusion pumps allow for

FIGURE 3 Screening of copolymer hydrogels to select top immune-resistant materials for further evaluation. (A) Polyacrylamide copolymer hydrogels were implanted in the subcutaneous space of mice for 28 days, upon which the tissues and gels were removed to examine foreign body response. (B) Representative sections of tissue and subsequent MT and H&E Staining. Scale bar represents 100 μm unless otherwise specified. (C) Fibrous capsule thickness of $n = 3$ samples (mean \pm s.d.) where each mean was determined from the median of 10 thicknesses per image. (D) Inflammation score determined by pathologists blinded to the test materials to characterize extent of inflammation.

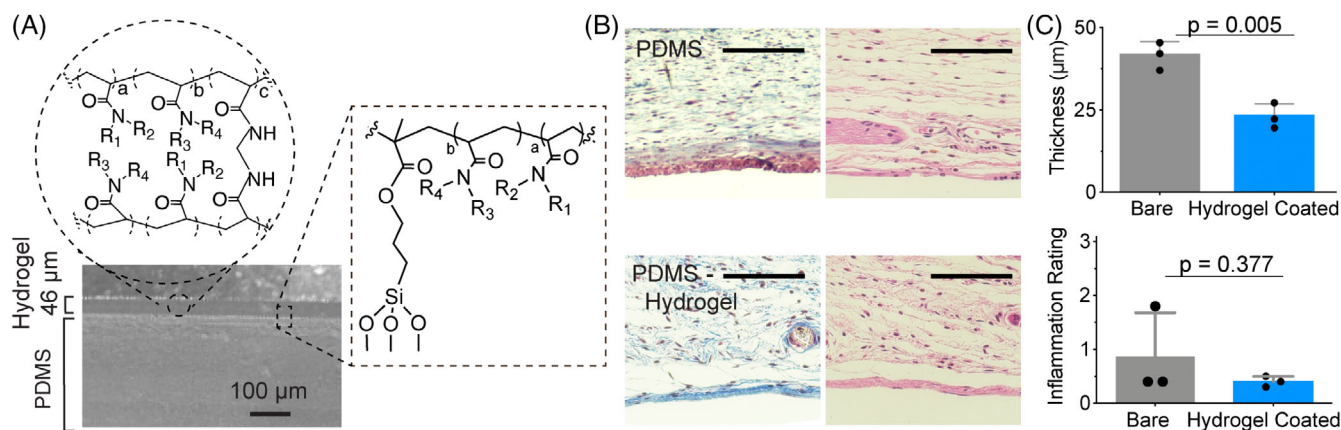


FIGURE 4 Demonstration of leading hydrogel coating on PDMS surfaces. (A) Homogenous coating of D5 copolymer hydrogels to PDMS visualized by SEM. (B) Representative images of MT (left) and H&E (right) staining of explanted hydrogels and adjacent tissues. Scale bar represents 100 μm . (C) Quantitative measurements of fibrosis (top), and semiquantitative inflammation scores as assigned by pathologists blinded to the test materials. Mean \pm s.d. significance from unpaired *t* test.

accurate and continuous delivery of therapeutic formulations, including clinical insulin formulations, allowing us to mimic the continuous basal administration of insulin into the subcutaneous tissue with a traditional infusion set catheter tip used clinically. Flow rate crucially impacts the lifetime and aggregation of proteins on a catheter tip. For humans, typical values of insulin dosing are in the range of 1 U/kg/day.³⁰ We therefore chose an insulin delivery rate of 0.25 $\mu\text{L}/\text{h}$ (0.025 U/h insulin) to mimic a similar basal rate. Because the standard tips of the Alzet[®] pumps are made of metal, we attached a silicone catheter tip to the pump tip to appropriately model clinical infusion sets. While PEG is often thought of as a “gold standard” anti-fouling material, PEG coatings are not used on current commercial insulin infusion sets. Furthermore, previous results from our lab indicate that over the timeframes evaluated, PEG-coated substrates do not outperform bare substrates.²⁴ These applied catheter tips were therefore either left uncoated (bare) or coated with our top-performing copolymer hydrogel D5 (Figure 5A). The coating of the silicon catheters was performed in a similar manner to PMDS disks described above, whereby catheters were plasma cleaned and coated with TMSPMA before a thin layer of prepolymer solution D5 was applied by dip-coating and subsequently photo-crosslinked to form a robust hydrogel coating. The process of applying this hydrogel coating was confirmed by FTIR analysis (Figure S5).

The pumps were then primed for 2 days at 37°C in phosphate buffered saline (PBS), per the manufacturer's instructions, and loaded with insulin lispro (Humalog, Eli Lilly) prior to subcutaneous implantation in a rat model of insulin-deficient diabetes (induced with streptozotocin, STZ). Following implantation, serum lispro concentrations were monitored by ELISA throughout the 28-day release period of the particular Alzet[®] pumps used in this study (Figure 5B). We sought to determine when the catheter tips occluded due to biofouling, resulting in pump failure. Upon occlusion, Alzet[®] pumps rupture, causing an immediate release of the remaining insulin and resulting in a spike in serum lispro levels³¹ (Figures 5D,E and S6). In these studies,

we defined a cutoff for excessive release of insulin at a serum insulin concentration of 10 mU/L based on literature reports (Figure 5D).^{32–34} While all pumps fitted with bare catheters failed within the 28-day study period, all D5-coated pumps remained functional and maintained consistent serum lispro levels. As the insulin infusion rate was chosen to simulate basal insulin dosing, there was no insulin coverage for carbohydrate consumption and thus blood glucose levels were not expected to reflect management of diabetes despite basal insulin infusion (Figures S7 and S8).

2.5 | Biocompatibility of osmotic insulin pumps

At the end of the 28-day study, implanted pumps were retrieved and physically evaluated (Figure 5C). While a thick fibrous capsule and aggregation was observed on bare catheter tips, notably less fibrosis was observed for D5 hydrogel-coated catheter tips. Tissue samples surrounding the tips, as well as the catheter tips themselves, were extracted for histological analysis and stained with MT, H&E, Congo Red, and immunostained for the macrophage cell marker CD68 (Figure 5F). MT staining demonstrated fibrous capsule formation around both bare and D5-coated catheter tips, and several populations of lymphocytes (eosinophils, monocytes, macrophages, and foreign body multinucleated cells) were observed around bare catheters. Notably, the region surrounding the bare catheter tips exhibited high levels of inflammation and high density of inflammatory cells (high prevalence of dark blue and purple staining). Moreover, fibroblasts in the region around the bare catheter tips had begun to align—as seen from their nuclear arrangement—as they formed the fibrous capsule around the implanted catheter. These characteristics were absent in D5-coated catheter tips.

Similarly, H&E staining indicated a significantly more inflamed immune response in the tissues surrounding the bare catheter tips than D5-coated catheter tips. Surrounding the bare catheter tips, clear

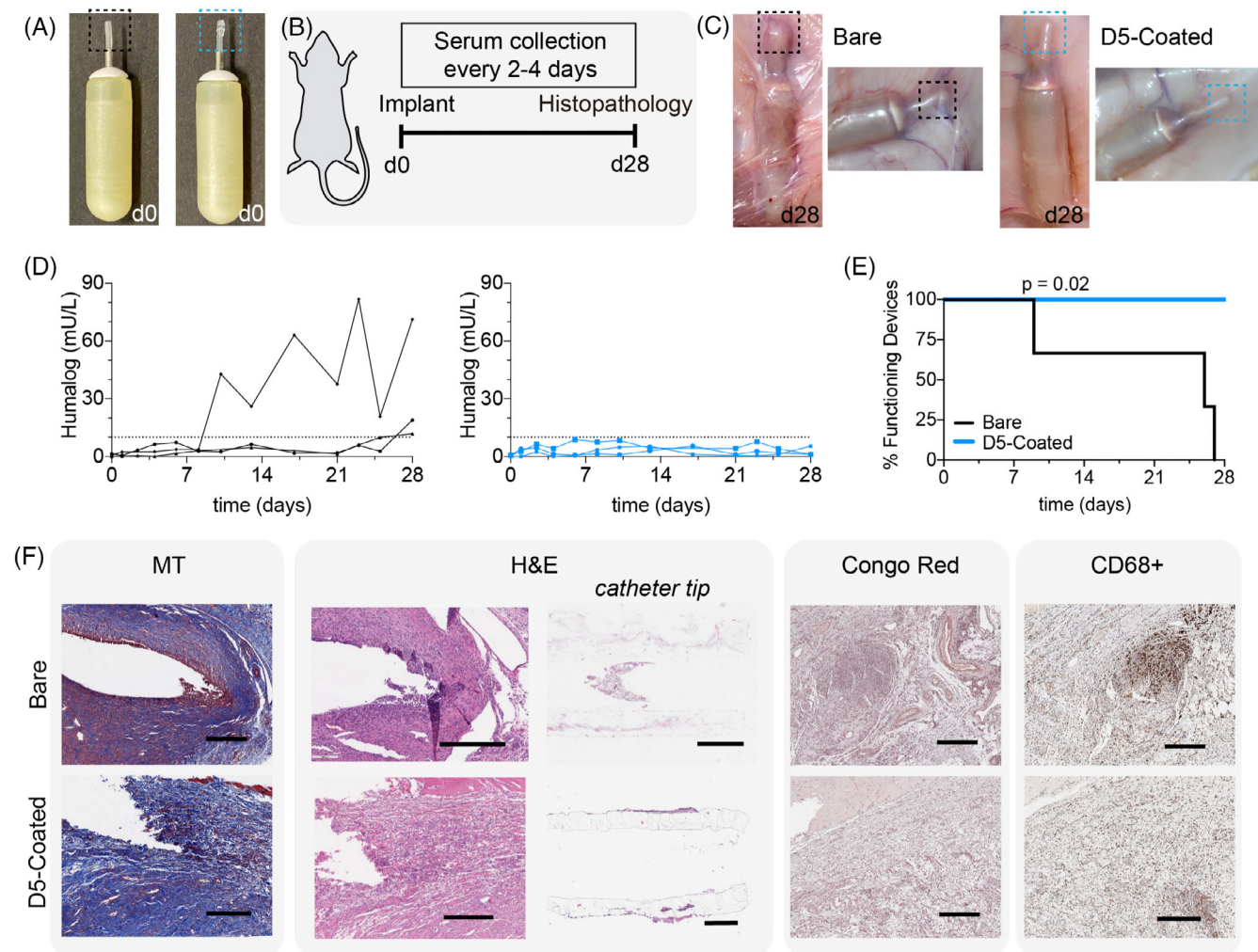


FIGURE 5 Application of leading hydrogel coating to osmotic insulin pumps. (A) Osmotic pumps with bare silicone tips (black) and D5-coated tips (blue) on implantable osmotic pumps. (B) Schematic of experimental timeline, whereby pumps were implanted in the dorsal region of diabetic rats, blood was collected over the course of 28 days, and pumps and tissues were explanted at the end of the study. (C) After 28 days, hydrogel coated pumps appear to have noticeably less fibrosis and protein aggregation. (D) Blood insulin values over time, determined by ELISA. (E) Pump survival curve demonstrating the timeframe over which pumps remain functional and consistently deliver insulin. Statistical significance of pump survival assessed with a Mantel–Cox test. (F) Immunostaining and histopathology of excised tissue and catheter tips. Scale bar represents 500 μm .

spaces indicated vessels from granulation tissues and capillary tissues, and there was fibrotic capsule formation with a thickness of $37 \pm 6 \mu\text{m}$ (mean \pm s.d. quantified across five locations). By contrast, surrounding the D5-coated catheter tips, the deposited collagen was found to be less mature (i.e., recently generated) as a thin fibrous capsule was beginning to form around the implant which could not be quantified. These D5-coated catheter tips also exhibited the presence of inflammatory cells (lymphocytes and macrophages), indicating that while the D5 hydrogel coating does not completely evade the FBR, it remarkably improved the biocompatibility of the implanted catheters.

In addition, the catheter tips themselves were cross-sectioned and stained, revealing the presence of immune cells on the inside of the bare catheter tips. This cellular accumulation inside the catheter tips could potentially be one driver of the occlusion of the pumps. By

contrast, cellular aggregation was not observed inside of the D5-coated catheter tip. Furthermore, Congo red staining indicated amyloid deposition, including from insulin. Aggregates were present in the area surrounding the bare catheter tips but were negligible in the areas surrounding the D5-coated tips. As macrophages dominate the FBR, CD68 staining was used as a general host immune cell marker to identify macrophages around the implant.³⁵ The presence of CD68 (macrophage) markers was notably reduced with the D5-coated catheter tips when compared with the bare catheter tips, with 24.5% of the tissue surrounding the bare catheter tips staining positive for CD68 compared with only 15.5% of the tissue surrounding the hydrogel-coated catheter tips (Figure 5F). Commensurate with the results discussed above, these studies indicate that coating of devices with select polyacrylamide-based copolymer hydrogels can reduce the FBR to them upon implantation in the body and improve their functional lifetime.

In these experiments, many factors were expected to contribute to the biocompatibility of the implants, including the presence of insulin, therefore Alzet[®] pumps filled with PBS were also evaluated for comparison (Figure S9). Insulin was found to aggravate the FBR to the implanted pumps, as pumps with either bare or D5-coated catheter tips delivering PBS infusion showed more mild inflammation and fewer immune cells than pumps delivering insulin. Similar to the results with insulin infusion described above, D-5-coated catheter tips exhibited improved biocompatibility over bare catheter tips when infusing PBS.

3 | DISCUSSION

In this work, we created a library of polyacrylamide-based copolymer hydrogel materials to develop novel coatings to improve the biocompatibility of implanted devices. While a number of coating technologies are currently used and many others are under development,^{36–39} including silver, heparin, and a variety of polyether hydrogels, each of these coatings face critical limitations that warrant the discovery of novel formulations that can be used on medical devices. Initially, we generated disks of each hydrogel formulation of interest, which were implanted in mice to screen their ability to mitigate fibrous capsule formation and reduce inflammation resulting from the FBR. We found that one polyacrylamide-based copolymer formulation, comprising a 50:50 mix of HEAm and MPAm, exhibited excellent biocompatibility following implantation into the subcutaneous tissue of mice over the course of 1 month. Moreover, when this hydrogel was applied to the surface of a PDMS implant, a notable reduction in fibrous capsule formation and local inflammation was observed at the interface of the implant, which was quantified by capsule thickness and assessed through pathological scoring by pathologists blinded to the test materials.

We also found that the HEAm-co-MPAm copolymer hydrogel can be used as a coating to extend the functional lifetime of insulin pumps in a rat model of T1D. Indeed, all insulin infusion pumps fitted with bare catheter tips occluded and failed within the 28-day study period, while all pumps fitted with catheters coated with our lead candidate hydrogels completely maintained their function. While pumps have been shown to improve glycemic control in people with diabetes,⁴⁰ the requirement that insulin infusion sets be replaced and moved to new locations in the subcutaneous tissue every few days is highly burdensome. The ability to prolong the functional lifetime of insulin infusion sets with a simple coating could dramatically improve the lives of people with diabetes.

Our leading candidate HEAm-co-MPAm copolymer hydrogel coatings notably improved the biocompatibility of the implanted pump systems by mitigating inflammation and the FBR. While the most desirable immune response to implanted materials is poorly understood and may depend on many application-specific parameters (e.g., tissue types at implantation site, the composition and mechanics of the implanted materials, and the infusion of therapeutics protein formulations to name a few), our studies indicate that our leading

copolymer hydrogels may provide a facile mechanism for improving the biocompatibility of a wide variety of medical materials. These polyacrylamide-based copolymer hydrogels can be even further tuned to optimize porosity and even nanotopography, which are known to effect engagement with immune cells.¹³ The facile tunability of these polyacrylamide coatings enables them to be more fully optimized for specific applications. Indeed, further optimization of these coatings on insulin infusion sets would best be conducted in diabetic swine, which are more representative of human skin anatomy and diabetes phenotype than the rat model of insulin-deficient diabetes used in the present study.⁴¹ Moreover, swine are also sufficiently large to enable the evaluation of full clinical insulin pumps and infusion sets over relevant timeframes. Overall, our findings can inform the design of facile surface modifications of implanted biomaterials for applications ranging from tissue-engineering to biosensors, and our lead candidate hydrogel compositions are promising for next-generation materials and implanted device development.

4 | CONCLUSION

In summary, by leveraging a combinatorial synthesis approach to generate a library of polyacrylamide-based copolymer hydrogels with excellent biocompatibility marked by reduced FBR and local inflammation. We were able to develop a simple-to-apply coating based on these materials that helps mitigate the FBR and improve tolerability of various implanted materials including insulin infusion set catheters. Through these studies we demonstrated that our leading candidate polyacrylamide-based copolymer hydrogel coatings have the potential to improve device function and lifetime, thereby reducing the burden of disease management for people regularly using implanted devices, such as those with diabetes.

5 | MATERIALS AND METHODS

5.1 | Materials

All materials were purchased from Sigma-Aldrich and used as received, unless specified otherwise.

5.2 | Hydrogel synthesis

Prepolymer formulations containing 20 wt % acrylamide monomers, 1 wt % lithium phenyl-2,4,6-trimethylbenzoylphosphinate (LAP) as photo-initiator, and 1 wt % *N,N'*-methylenebis(acrylamide) were mixed in distilled water and pipetted between two glass slides separated by a silicone spacer (0.25 mm ± 0.05 mm). Gels were crosslinked in a Luzchem photoreactor system with 8 W bulbs and an intensity of 25–40 W/m² (LZC-4, $h\nu = 365$ nm, 15 min). Hydrogels were placed in 1× PBS for at least 24 h before being punched with a 6 mm biopsy punch. All 2-acrylamido-2-methyl-propane sulfonic acid (AMPsAm)

formulations were made with slightly basic solution of 2:3 1 M NaOH:water. [tris(hydroxymethyl)methyl]acrylamide (tHMAM) formulations were made with 50:50 dimethylformamide:water as well as 100% *N*-isopropylacrylamide (NiPAm), 75% diethylacrylamide (DEAm), 25% NiPAm, and 25% hydroxymethylacrylamide (HMAM), 75% NiPAm. PMPC hydrogels was prepared as described previously.^{15,26} Briefly, polyzwitterionic hydrogels were prepared with monomeric solutions in 1 M NaCl with 4% *N,N'*-methylenebisacrylamide (MBAm) crosslinker. A stock solution of 15% sodium metabisulfite and 40% ammonium persulfate was added to the prepolymer solution at ~1 wt % and polymerization was initiated at 60°C. PEG hydrogels were prepared similarly with a prepolymer solution of 15 wt % PEG diacrylate (M_n 780²⁷⁻²⁹) and 5 wt % PEG acrylate (M_n 480).

5.3 | Platelet adhesion assay

Platelet assay was performed as described previously.³⁰ Briefly, 6 mm punches of hydrogels were incubated for 24 h at 37°C with 50% fetal bovine serum. Then, whole rat blood was mixed with acid citrate dextrose anticoagulant buffer for the preparation of PRP. PRP was obtained via centrifugation at 600g for 10 min at 10°C. Platelets were diluted to 2.5×10^6 platelets/mL in 1× PBS. 100 μL of the platelet rich plasma was incubated for 1 h on hydrogel surfaces. Platelets were rinsed with 1× PBS and fixed with 4% paraformaldehyde (PFA). Hydrogel surfaces were imaged with an EVOS XL Core Imaging System microscope (Life Technologies).

5.4 | Hydrogel coating of polydimethylsiloxane disks

Sylgard 184 (Dow) was mixed in 10:1 ratio of monomer:crosslinker and cured at 100°C for 45 min per manufacturer instructions. Hydroxyl groups were activated on the surface of PDMS after 3 min of O₂/Ar plasma and TMSPMA pipetted directly on the surface of PDMS and allowed to react for 10 min. TMSPMA-coated PDMS disks were then rinsed three times with deionized water and dried with N₂. TMSPMA-coated PDMS disks were then soaked in prepolymer formulation overnight prior to spin coating, which was conducted at 500 rpm for 30 s. The prepolymer coatings were then polymerized at 365 nm for 15 min. Hydrogel-coated PDMS disks were then rinsed three times with deionized water and stored in deionized water.

5.5 | Scanning electron microscopy

SEM images were acquired with an FEI Magellan 400 XHR Microscope with a Beam Voltage of 1 kV and 30 μs dwell time. The sample was pressed onto carbon paint and sputter-coated with Au:Pd (60:40) before imaging. Quantification of sample parameters was taken from a minimum of five different areas and reported as mean ± s.d.

5.6 | Ethical approval of animal studies

Animal studies were performed in accordance with the guidelines for the care and use of laboratory animals. All protocols were approved by the Stanford Administrative Panel on Laboratory Animal Care (APLAC-32109; APLAC-32873) and were conducted in accordance with National Institutes of Health guidelines.

5.7 | In vivo mouse biocompatibility

Six to eight weeks old female B57BL/6 mice were purchased from Charles River Laboratories (Wilmington, MA). Subcutaneous implantations (two per mouse, one on each side of the mouse, and at least 2 cm from point of incision) were made on the dorsal region on mice. Longitudinal incisions (<2 cm) on the dorsal region was made to access the subcutaneous space. Pockets on either side of the incision were made with a blunt spatula for implanting the materials, one on each side. Incisions were sutured and mice monitored for signs of distress. After 28 days following implantation, mice were euthanized by CO₂ asphyxiation. The hydrogel and surrounding tissues were harvested ($n = 3$ for each unique sample) and the tissue was fixed for 48 h in 4% PFA.

5.8 | Histology

Fixed tissues were embedded in paraffin and processed by Animal Histology Services at Stanford University. 4 μm cross-sections were stained using MT and H&E staining using standard methods. Photographs were taken with EVOS FL Cell Imaging System (Thermo Fisher Scientific) at various magnifications. Rat tissues fixed with 10% formalin for 72 h and stored in 70% ethanol. Tissues were processed by Histowiz (Brooklyn, NY), fixed in paraffin, sectioned into 5 μm slides, and stained for MT, H&E, anti-CD68 (Abcam, ab125212), and Congo Red.

5.9 | Pathological ranking

The thickness for the collagen layer (blue) and pseudosynovium layer (red/purple) were analyzed using ImageJ software, taking the median of 10 measurements per sample. While H&E staining provides a qualitative assay to assess fibrotic response, we sought to quantify the extent to which the hydrogels elicited an immune response. Two pathologists blinded to the test materials graded each H&E-stained sample ($n = 3$ for each hydrogel sample), providing a rating between 0 (little to no inflammatory response) to 3 (severe inflammation), with assessment based on the prevalence of various immune cells at the lining between the skin and implant. Rating was multiplied by area of proportion of impacted area.

5.10 | Streptozotocin-induced model of diabetes in rats

Animal studies were performed in accordance with the guidelines for the care and use of laboratory animals; all protocols were approved by the Stanford Institutional Animal Care and Use Committee. Male Sprague Dawley rats (Charles River) were used for experiments. The protocol used for STZ induction adapted from the protocol by Wu and Huan.⁴⁰ Briefly, male Sprague Dawley rats 160–230 g (8–10 weeks) were weighed and fasted 6–8 h prior to treatment with STZ. STZ was diluted to 10 mg/mL in the sodium citrate buffer immediately before injection. STZ solution was injected into the intraperitoneal space at 65 mg/kg into each rat. Rats were provided with water containing 10% sucrose for 24 h after injection with STZ. Rat blood glucose levels were tested for hyperglycemia daily after the STZ treatment via tail vein blood collection using a handheld Bayer Contour Next glucose monitor (Bayer). Diabetes was defined as having three consecutive blood glucose measurements >400 mg/dL in nonfasted rats.

5.11 | Preparation of osmotic pumps

Commercial Humalog (Eli Lilly) formulations composed of glycerol (1.6%), meta-cresol (0.315%), dibasic sodium phosphate (0.188%), and zinc (0.00197%) were purchased and used as received. Alzet osmotic pumps (Durect Corporation, Model 2004) were filled with ~200 μ L Humalog per the manufacturer's instructions. Pumps had a release rate of 0.25 μ L/h (0.025 U/h of Humalog). Prefilled pumps were placed in sterile saline at 37°C for 48 h prior to animal implants. For all pumps, 8 mm of RenaSil silicone rubber tubing (Braintree Scientific, SILO37) was attached to the tip of the pumps, due to facile modification of silicone. Hydrogel coated silicone tips were prepared by O₂/Ar plasma for 3 min and immersed in solution of TMSPPMA for 1 h, followed by incubation in prepolymer solution for 24 h. Hydrogel prepolymer solution was pipetted on the tip of the pump and crosslinked for 3 min in a Luzchem photoreactor system with 8 W bulbs and an intensity of 25–40 W/m² (LZC-4, $h\nu = 365$ nm).

5.12 | In vivo implantation of osmotic pumps

Following diabetes induction, osmotic pumps were implanted into the diabetic rats. Skin incisions were made on the dorsal region of the rat. A blunt spatula was used to open a pocket in the subcutaneous space. Pumps were inserted and incision closed with 4–0 suture. None displayed visible signs of inflammation or infection throughout the study. After 28 days, animals were euthanized by exsanguination and osmotic pumps and tissue samples were collected.

5.13 | Blood glucose and Humalog quantification

One drop of blood was collected at specified time points via tail vein blood collection onto Contour (R) Next One Blood Glucose

Monitoring System. For determining insulin levels, 60 μ L of blood was collected at specified time points via tail vein blood collection into serum-gel microtubes (Sarstedt 50–809–211). Tubes were centrifuged for 5 min to extract serum and stored at –80°C. Serum insulin concentrations were determined with Northern Lights Mercodia Lispro NL-ELISA (Mercodia AB, 10-1291-01) according to manufacturer's instructions, using 10 μ L of undiluted serum for each time point. Luminescence was measured in a Synergy H1 Microplate Reader (BioTek). Concentrations were calculated from the generated standard curves.

5.14 | Statistical analysis

All implants were conducted with $n = 3$ mice or rats. Unless otherwise specified, measurements are reported as mean \pm standard deviation and analyzed with Prism Graphpad v9.0.0.

AUTHOR CONTRIBUTIONS

Doreen Chan, Caitlin L. Maikawa, and Eric A. Appel designed experiments. Doreen Chan, Caitlin L. Maikawa, Andrea I. d'Aquino, and Eric A. Appel conducted experiments. Doreen Chan, Caitlin L. Maikawa, Andrea I. d'Aquino, Shyam S. Raghavan, Megan L. Troxell, and Eric A. Appel analyzed data. Doreen Chan, Caitlin L. Maikawa, Shyam S. Raghavan, Megan L. Troxell, and Eric A. Appel wrote the paper.

ACKNOWLEDGMENTS

This work was funded in part by NIDDK R01 (NIH grant #R01DK119254) and a Pilot and Feasibility funding from the Stanford Diabetes Research Center (NIH grant #P30DK116074) and the Stanford Child Health Research Institute, as well as the American Diabetes Association Grant (1-18-JDF-011) and a Research Starter Grant from the PhRMA Foundation. Caitlin L. Maikawa was supported by the NSERC Postgraduate Scholarship and the Stanford BioX Bowes Fellowship. We thank the Stanford Animal Histology Services and Histowiz for help with processing of histologic specimens. We thank Dr. José Vilches-Moure (Comparative Medicine, Stanford University) for invaluable discussion on histology images.

CONFLICT OF INTEREST STATEMENT

Doreen Chan and Eric A. Appel are listed as authors on a provisional patent application describing the technology reported in this article.

DATA AVAILABILITY STATEMENT

The data that support the findings of this study are available on request from the corresponding author. The data are not publicly available due to privacy or ethical restrictions.

ORCID

Caitlin L. Maikawa  <https://orcid.org/0000-0002-6214-1226>

Andrea I. d'Aquino  <https://orcid.org/0000-0002-4204-8219>

Eric A. Appel  <https://orcid.org/0000-0002-2301-7126>

REFERENCES

- Ratner BD. A paradigm shift: biomaterials that heal. *Polym Int*. 2007; 56(10):1183-1185.
- Prakasam M, Locs J, Salma-Ancane K, Loca D, Largeteau A, Berzina-Cimдина L. Biodegradable materials and metallic implants—a review. *J Funct Biomater*. 2017;8(4):44.
- Saini M, Singh Y, Arora P, Arora V, Jain K. Implant biomaterials: a comprehensive review. *World J Clin Cases*. 2015;3(1):52-57.
- Gray M, Meehan J, Ward C, et al. Implantable biosensors and their contribution to the future of precision medicine. *Vet J*. 2018;239:21-29.
- Thevenot P, Hu W, Tang L. Surface chemistry influences implant biocompatibility. *Curr Top Med Chem*. 2008;8:270-280.
- Blaszkiowski C, Sheikh S, Thompson M. Biocompatibility and anti-fouling: is there really a link? *Trends Biotechnol*. 2014;32(2):61-62.
- Wilson CJ, Clegg RE, Leavesley DI, Pearcy MJ. Mediation of biomaterial–cell interactions by adsorbed proteins: a review. *Tissue Eng*. 2005;11(1/2):1-18.
- Sheikh Z, Brooks P, Barzilay O, Fine N, Glogauer M. Macrophages, foreign body Giant cells and their response to implantable biomaterials. *Materials*. 2015;8(9):5671-5701.
- Ward WK. A review of the foreign-body response to subcutaneously-implanted devices: the role of macrophages and cytokines in biofouling and fibrosis. *J Diabetes Sci Technol*. 2008;2(5):768-777.
- Lilly E. Humalog (insulin lispro) [package insert]. U.S. Food and Drug Administration. Revised March 2013. Accessed April 16, 2020 https://www.accessdata.fda.gov/drugsatfda_docs/label/2013/020563s115lbl.pdf
- Hauzenberger JR, Munzker J, Kotzbeck P, et al. Systematic in vivo evaluation of the time-dependent inflammatory response to steel and Teflon insulin infusion catheters. *Sci Rep*. 2018;8(1):1132.
- Damodaran VB, Murthy NS. Bio-inspired strategies for designing anti-fouling biomaterials. *Biomater Res*. 2016;20:18.
- Desai T, Shea LD. Advances in islet encapsulation technologies. *Nat Rev Drug Discov*. 2017;16(5):338-350.
- Veiseh O, Doloff JC, Ma M, et al. Size- and shape-dependent foreign body immune response to materials implanted in rodents and non-human primates. *Nat Mater*. 2015;14(6):643-651.
- Zhang L, Cao Z, Bai T, et al. Zwitterionic hydrogels implanted in mice resist the foreign-body reaction. *Nat Biotechnol*. 2013;31(6):553-556.
- Zhang P, Sun F, Tsao C, et al. Zwitterionic gel encapsulation promotes protein stability, enhances pharmacokinetics, and reduces immunogenicity. *Proc Natl Acad Sci*. 2015;112(39):12046-12051.
- Xie X, Doloff JC, Yesilyurt V, et al. Reduction of measurement noise in a continuous glucose monitor by coating the sensor with a zwitterionic polymer. *Nat Biomed Eng*. 2018;2(12):894-906.
- Hunter JM, Jaeger SH, Matsui T, Miyaji N. The pseudosynovial sheath—its characteristics in a primate model. *J Hand Surg Am*. 1983; 8(4):461-470.
- MacCallum N, Howell C, Kim P, et al. Liquid-infused silicone As a biofouling-free medical material. *ACS Biomater Sci Eng*. 2014;1(1): 43-51.
- Mehta RI, Mehta RI. Hydrophilic polymer embolism: implications for manufacturing, regulation, and Postmarket surveillance of coated intravascular medical devices. *J Patient Saf*. 2019;17:e1069.
- Chang C-J, Chen C-H, Chen B-M, et al. A genome-wide association study identifies a novel susceptibility locus for the immunogenicity of polyethylene glycol. *Nat Commun*. 2017;8(1):522.
- Harding JA, Engbers CM, Newman MS, Goldstein NI, Zalipsky S. Immunogenicity and pharmacokinetic attributes of poly(ethylene glycol)-grafted immunoliposomes. *Biochim Biophys Acta*. 1997; 1327(2):181-192.
- Hoang Thi TT, Pilkington EH, Nguyen DH, Lee JS, Park KD, Truong NP. The importance of poly(ethylene glycol) alternatives for overcoming PEG immunogenicity in drug delivery and bioconjugation. *Polymers (Basel)*. 2020;12(2):298.
- Chan D, Chien J-C, Axpe E, et al. Combinatorial polyacrylamide hydrogels for preventing biofouling on implantable biosensors. *Adv Mater*. 2022;34(24):2109764.
- Zhang H, Chiao M. Anti-fouling coatings of poly(dimethylsiloxane) devices for biological and biomedical applications. *J Med Biol Eng*. 2015;35(2):143-155.
- Hegggers JP, Kossovsky N, Parsons RW, Robson MC, Pelley RP, Raine TJ. Biocompatibility of silicone implants. *Ann Plast Surg*. 1983;11(1):38-45.
- Colas A, Curtis J. Silicone biomaterials: history and chemistry & medical applications of silicones. In: Ratner BD, Hoffman AS, Schoen FJ, Lemons JE, eds. *Biomaterials Science: An Introduction to Materials in Medicine*. Elsevier Academic Press; 2004 80-86, 697-707.
- Prantl L, Schreml S, Fichtner-Feigl S, et al. Clinical and morphological conditions in capsular contracture formed around silicone breast implants. *Plast Reconstr Surg*. 2007;120(1):275-284.
- Franca DC, de Castro AL, Soubhia AM, de Aguiar SM, Goiato MC. Evaluation of the biocompatibility of silicone gel implants - histomorphometric study. *Acta Inform Med*. 2013;21(2):93-97.
- Grant CW, Duclos SK, Moran-Paul CM, et al. Development of standardized insulin treatment protocols for spontaneous rodent models of type 1 diabetes. *Comp Med*. 2012;62(5):381-390.
- Herrlich S, Spieth S, Messner S, Zengerle R. Osmotic micropumps for drug delivery. *Adv Drug Deliv Rev*. 2012;64(14):1617-1627.
- Kolewe KW, Peyton SR, Schiffman JD. Fewer bacteria adhere to softer hydrogels. *ACS Appl Mater Interfaces*. 2015;7(35):19562-19569.
- Miyazaki M, Mukai H, Iwanaga K, Morimoto K, Kakemi M. Pharmacokinetic-pharmacodynamic modelling of human insulin: validity of pharmacological availability as a substitute for extent of bioavailability. *J Pharm Pharmacol*. 2010;53(9):1235-1246.
- Modulevsky DJ, Cuerrier CM, Pelling AE. Biocompatibility of subcutaneously implanted plant-derived cellulose biomaterials. *PLoS One*. 2016;11(6):e0157894.
- van Putten SM, Ploeger DTA, Popa ER, Bank RA. Macrophage phenotypes in the collagen-induced foreign body reaction in rats. *Acta Biomater*. 2013;9(5):6502-6510.
- Schierholz JM, Lucas LJ, Rump A, Pulverer G. Efficacy of silver-coated medical devices. *J Hosp Infect*. 1998;40(4):257-262.
- Biran R, Pond D. Heparin coatings for improving blood compatibility of medical devices. *Adv Drug Deliv Rev*. 2017;112:12-23.
- Kim BS, Hrkach JS, Langer R. Biodegradable photo-crosslinked poly(ether-ester) networks for lubricious coatings. *Biomaterials*. 2000; 21(3):259-265.
- Cyphert EL, von Recum HA. Emerging technologies for long-term antimicrobial device coatings: advantages and limitations. *Exp Biol Med*. 2017;242(8):788-798.
- Wu KK, Huan Y. Streptozotocin-induced diabetic models in mice and rats. *Curr Protoc Pharmacol*. 2008;40(1):5.47.1-5.47.14.
- Maikawa CL, Smith AAA, Zou L, et al. A co-formulation of supramolecularly stabilized insulin and pramlintide enhances mealtime glucagon suppression in diabetic pigs. *Nat Biomed Eng*. 2020;4(5):507-517.

SUPPORTING INFORMATION

Additional supporting information can be found online in the Supporting Information section at the end of this article.

How to cite this article: Chan D, Maikawa CL, d'Aquino AI, Raghavan SS, Troxell ML, Appel EA. Polyacrylamide-based hydrogel coatings improve biocompatibility of implanted pump devices. *J Biomed Mater Res*. 2023;1-11. doi:10.1002/jbm.a.37521